

Innovation in InSAR Processing and Analysis of C-, X- and L-Band SAR Data for Natural Hazards, Agriculture, Marine and Coastal Applications in the framework of ASI's "Multi-Mission and Multi-Frequency SAR" Program

Deodato Tapete, Antonio Montuori, Fabrizio Lenti, Patrizia Sacco, Maria Virelli, Simona Zoffoli, Alessandro Coletta

Italian Space Agency (ASI)

FRINGE 2023

University of Leeds, UK | 11 - 15 September 2023



Agenzia Spaziale Italiana

Sensor-specific R&D program: Multi-mission & multi-frequency SAR

- **10 R&D projects** (from April 2021 to July 2023) about methods, techniques & algorithms for *exploitation* of multi-mission & multi-frequency SAR data, also integrated with other types of EO and/or non-EO data
- **Focus on L-band SAR (e.g. SAOCOM)**, also in relation to ASI-CONAE SIASGE cooperation
- **Pre-operational projects**, based on innovative ideas & algorithms, with credible perspectives of engineering and pre-operational development
- Update the background and needs of the SAR user community to support and define **medium-to-long term strategies** of new EO applications
- In turn, enable user-driven applications → **scientific downstream**
- Support the SAR-based research activities carried out by public and private national community – **also in cooperation with international partners** –, contributing to maintain a leading position within the international context



R&D areas of specific interest & ASI projects

Agriculture

- SARAGRI
- CLEXIDRA
- MultiBigSARData



Urban areas

- MultiBigSARData



Natural hazards

- MUSAR
- MEFISTO
- DInSAR-3M



Cryosphere

- CRIOSAR
- SMIVIA



Sea & coast

- APPLICAVEMARS
- COAST



Validation of products generated from multi-frequency SAR data by using ground-truth data

ASI's Multi-mission & multi-frequency SAR projects @ FRINGE 2023 – Part 1



Where and when you can hear about ASI's Multi-mission & multi-frequency SAR projects @ FRINGE 2023

2.03.a: Ice and Snow 2

Time: 12/Sept/2023: 2:00pm-3:40pm · Location: Auditorium I

CRIOSAR

3:00pm - 3:20pm

Oral_20

Assessing Rock Glacier Activity In Val Senales By Exploiting Multiband SAR Data Through Differential SAR Interferometry And Offset Tracking

Fabio Bovenga¹, Ilenia Argentiero¹, Antonella Belmonte¹, Alberto Refice¹, Giovanni Cuzzo², Melisa Soledad Heredia², Mattia Callegari², Claudia Notarnicola², Davide Oscar Nitti³, Raffaele Nutricato³

¹Institute for Electromagnetic Sensing of the Environment, National Research Council of Italy (CNR-IREA); ²EURAC Research - Institute for Earth Observation; ³GAP s.r.l.

POSTER SESSION

Time: 12/Sept/2023: 4:30pm-7:00pm · Location: Poster Session/Exhibition

CRIOSAR

Multi-band SAR Interferometry For Snow Water Equivalent Estimation Over Alpine Mountains

Fabio Bovenga¹, Antonella Belmonte¹, Alberto Refice¹, Ilenia Argentiero¹, Simone Pettinato², Emanuele Santi², Simonetta Paloscia²

¹Institute for Electromagnetic Sensing of the Environment, National Research Council of Italy (CNR-IREA); ²Institute of Applied Physics, National Research Council of Italy (IFAC-CNR)

POSTER SESSION

Time: 12/Sept/2023: 4:30pm-7:00pm · Location: Poster Session/Exhibition

MUSAR

"The Data Fusion Application for a Multifrequency Post-processing Analysis of A-DInSAR Data"

Niccolò Belcecchi¹, Gianmarco Pantozzi¹, Carlo Alberto Stefanini¹, Paolo Mazzanti^{1,2}, Alessandro Brunetti¹, Michele Gaeta¹

¹NHAZCA Srl, Via V. Bachelet 12, Rome 00185, Italy; ²Dipartimento di Scienze della Terra, Università degli studi di Roma "La Sapienza", Piazzale Aldo Moro 5, Rome 00185, Italy



ASI's Multi-mission & multi-frequency SAR projects @ FRINGE 2023 – Part 2



Where and when you can hear about ASI's Multi-mission & multi-frequency SAR projects @ FRINGE 2023

5.01.a: C-and L-band synergies: ESA-JAXA cooperation and beyond **DInSAR-3M**

Time: 15/Sept/2023: 9:00am-10:40am · Location: Auditorium I

Oral_20

On the P-SBAS Processing Chain New Developments For The Generation Of SAOCOM-1 Advanced DInSAR Products

Claudio De Luca¹, Yenni Lorena Belen Roa¹, Manuela Bonano¹, Francesco Casu¹, Leonardo Euillades², Pablo Euillades², Marianna Franzese¹, Michele Manunta¹, Yasir Muhammad¹, Giovanni Onorato¹, Pasquale Striano¹, Ivana Zinno¹, Riccardo Lanari¹

¹Istituto per il Rilevamento Elettromagnetico dell'Ambiente (IREA), CNR, Napoli, Italy; ²Conicet, Instituto CEDIAC, Facultad de Ingeniería, Universidad Nac de Cuyo, Mendoza, Argentina



Facilitated accessibility to satellite SAR data

COSMO-SkyMed First & Second Generation (CSK & CSG)

- New portal for institutional users (<https://portal.cosmo-skymed.it/CDMFE/home>)
- Opportunity to task CSG to concatenate temporally and spatially with existing archive CSK images, and thus achieve observation continuity
- Over Italy, through MapItaly Project

Mission	Satellite	Sensor	Sensor Mode	Sensor Type	Collection	Product Status	Sensing Start	Sensing Stop	Orbit Direction	Swath	Polarization	Look Side	NearRangeIncidenceAngle
CSK	CSK1	SAR	STRIPMAP	RADAR	LI_SAR1	ARCHIVED	10-Jan-2022 09:24:18.071	10-Jan-2022 09:24:23.430	ASCENDING	57R-008	HH	RIGHT	30916
CSK	CSK1	SAR	STRIPMAP	RADAR	LI_SAR1	ARCHIVED	10-Jan-2022 09:23:01.921	10-Jan-2022 09:23:07.220	ASCENDING	57R-002	HH	RIGHT	21940
CSK	CSK1	SAR	STRIPMAP	RADAR	LI_SAR1	ARCHIVED	10-Jan-2022 09:23:47.784	10-Jan-2022 09:23:55.094	ASCENDING	57R-003	HH	RIGHT	24038
CSK	CSK1	SAR	STRIPMAP	RADAR	LI_SAR1	ARCHIVED	09-Jan-2022 04:48:03.833	09-Jan-2022 04:47:30.381	ASCENDING	57R-007	HH	RIGHT	32060
CSK	CSK1	SAR	STRIPMAP	RADAR	LI_SAR1	ARCHIVED	09-Jan-2022 18:50:08.083	09-Jan-2022 18:51:54.830	DESCENDING	57R-006	HH	RIGHT	30500
CSK	CSK1	SAR	STRIPMAP	RADAR	LI_SAR1	ARCHIVED	09-Jan-2022 18:50:28.468	09-Jan-2022 18:50:38.080	DESCENDING	57R-003	HH	RIGHT	24800
CSK	CSK1	SAR	SPOTLIGHT-OC	RADAR	LI_SAR1	ARCHIVED	09-Jan-2022 18:50:06.740	09-Jan-2022 18:50:11.170	DESCENDING	52C-039	HH	RIGHT	64546
CSK	CSK1	SAR	STRIPMAP	RADAR	LI_SAR1	ARCHIVED	09-Jan-2022 18:49:59.970	09-Jan-2022 18:49:52.797	DESCENDING	57R-003	HH	RIGHT	24730
CSK	CSK1	SAR	STRIPMAP	RADAR	LI_SAR1	ARCHIVED	09-Jan-2022 09:05:41.070	09-Jan-2022 09:05:48.947	ASCENDING	57R-005	HH	RIGHT	27716
CSK	CSK1	SAR	SPOTLIGHT-OC	RADAR	LI_SAR1	ARCHIVED	09-Jan-2022 09:05:39.174	09-Jan-2022 09:05:54.471	ASCENDING	52C-035	HH	RIGHT	61784
CSK	CSK1	SAR	SPOTLIGHT-OC	RADAR	LI_SAR1	ARCHIVED	09-Jan-2022 09:05:39.174	09-Jan-2022 09:05:54.471	ASCENDING	52C-035	HH	RIGHT	61784
CSK	CSK1	SAR	STRIPMAP	RADAR	LI_SAR1	ARCHIVED	09-Jan-2022 09:04:47.329	09-Jan-2022 09:04:59.615	ASCENDING	57R-007	HH	RIGHT	11602
CSK	CSK1	SAR	STRIPMAP	RADAR	LI_SAR1	ARCHIVED	09-Jan-2022 18:33:13.261	09-Jan-2022 18:33:20.818	DESCENDING	57R-002	HH	RIGHT	21923
CSK	CSK1	SAR	STRIPMAP	RADAR	LI_SAR1	ARCHIVED	09-Jan-2022 18:33:37.716	09-Jan-2022 18:33:45.880	DESCENDING	57R-008	HH	RIGHT	27716
CSK	CSK1	SAR	STRIPMAP	RADAR	LI_SAR1	ARCHIVED	09-Jan-2022 18:31:48.855	09-Jan-2022 18:33:08.640	DESCENDING	57R-003	HH	RIGHT	24777
CSK	CSK1	SAR	SPOTLIGHT-OB	RADAR	LI_SAR1	ARCHIVED	09-Jan-2022 04:43:28.046	09-Jan-2022 04:43:38.171	ASCENDING	52B-037	VH	RIGHT	83002
CSK	CSK1	SAR	STRIPMAP	RADAR	LI_SAR1	ARCHIVED	09-Jan-2022 04:43:09.839	09-Jan-2022 04:43:10.999	ASCENDING	57R-003	HH	RIGHT	24600
CSK	CSK1	SAR	SPOTLIGHT-OB	RADAR	LI_SAR1	ARCHIVED	09-Jan-2022 04:43:09.840	09-Jan-2022 04:43:10.171	ASCENDING	52B-037	VH	RIGHT	83002

SAOCOM

- New dedicated ASI portal (<http://saocom.asi.it:8081>)
- Data dissemination over the “Zone of Exclusivity” (ZoE; 10W-50E longitude range and 30-80N latitude range), currently via:
 - Archive imagery provision service
 - Beta-testing for ordering new acquisitions & products
- The experience led to current systematic acquisition plan over Italy and Europe

SAOCOM Data Hub

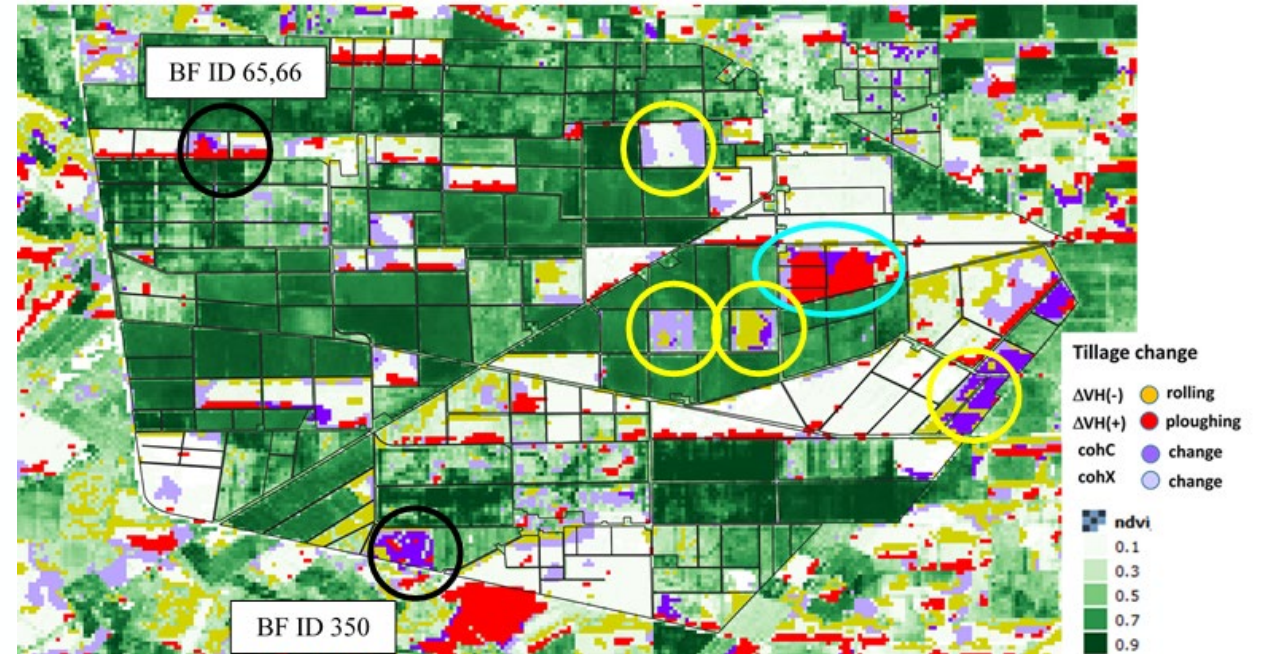
Display 1 to 25 of 346 products. Order By: Ingestion Date. 0 products selected.

Request Done: { footprint:Intersects(POLYGON((-0.637565054422137 35.99070424440099.37 33564091453906 ...))

- EDL SARL EOL1ASARSAO1A1189872
- EDL SARL EOL1ASARSAO1A1189951
- EDL SARL EOL1ASARSAO1A1189844
- EDL SARL EOL1ASARSAO1A119348
- EDL SARL EOL1ASARSAO1A115339

Achievements in CSK & CSG data exploitation

- Total amount of products provided as of July 2023: [5787](#) (5045 archive and 742 new tasking)
- Mostly in StripMap mode, single pol, for interferometric and change detection analyses
- CSG satellites also tasked to collect series of quad-pol StripMap images to test the enhanced polarimetric capabilities compared to what previously allowed by CSK, e.g. for maritime applications.
- Furthermore, by adding CSG satellites into the MapItaly Project since nearly the beginning of the program, the temporal revisit at X-band was much improved **up to 1 day (tandem pairs)**. Benefits for time-sensitive applications or requiring higher frequency of observations.

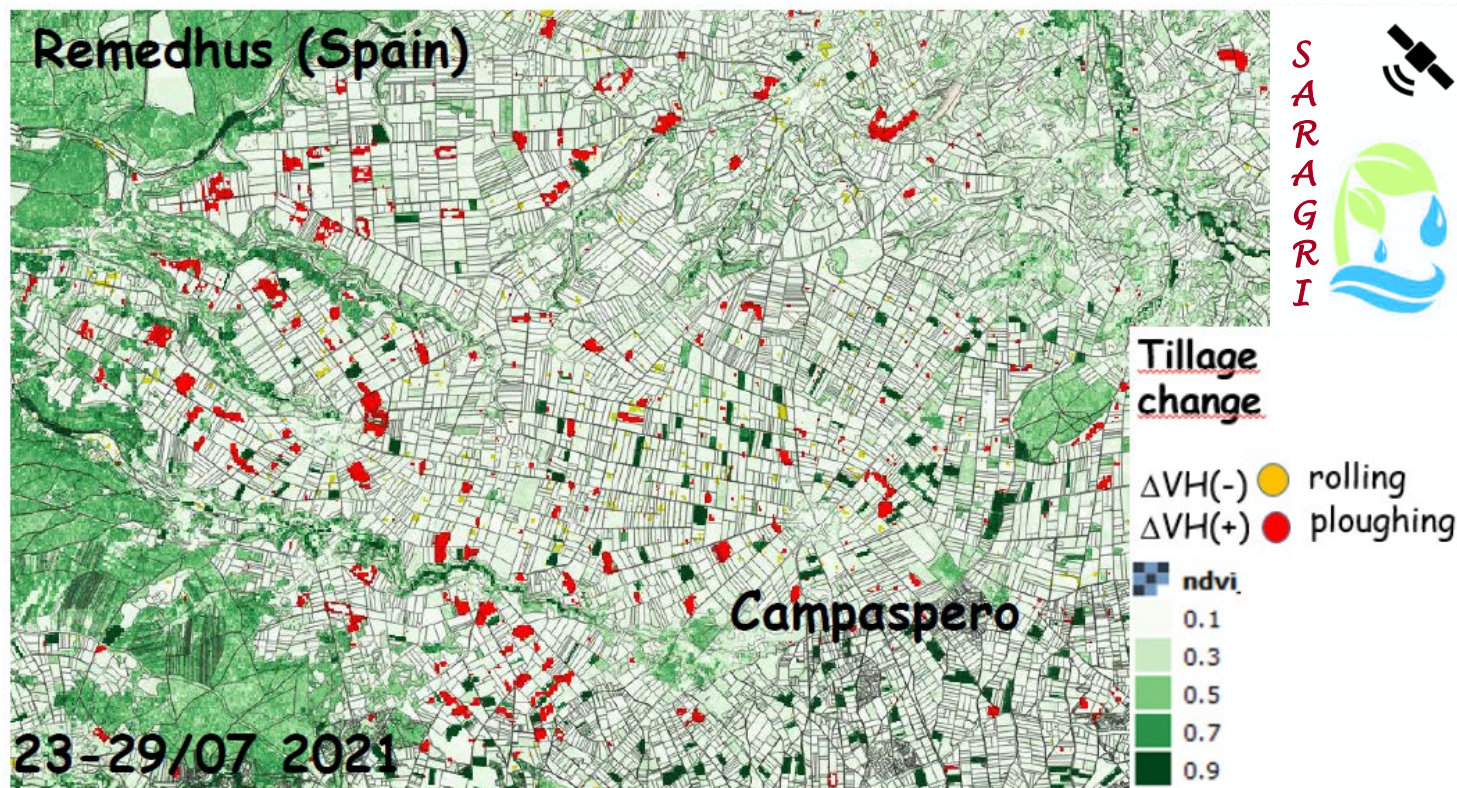


Tillage change map over Jolanda di Savoia based on a 2-day revisit CSG-CSK pair, where X-band coherence improves the detection of known tillage events (black circles) and identifies additional areas (light purple) compared to C-band 6-day Sentinel-1 coherence (**image courtesy: CNR-IREA, SARAGRI project**).

SARAGRI: S1 tillage change detection

- Original algorithm (Satalino et al., 2018) incoherent change detection applied to S1- cross-pol over bare soils
- Multi-scale approach to separate precipitation effects (medium-scale) on backscatter.

Example of tilled/non-tilled fields by S1 cross-pol change and S-2 NDVI (≤ 0.3) @100m scale



Satalino *et al.* (2018) "Sentinel-1 & Sentinel-2 Data for Soil Tillage Change Detection," *IGARSS 2018 - 2018 IEEE International Geoscience and Remote Sensing Symposium*, Valencia, Spain, 2018, pp. 6627-6630, doi: 10.1109/IGARSS.2018.8519103.

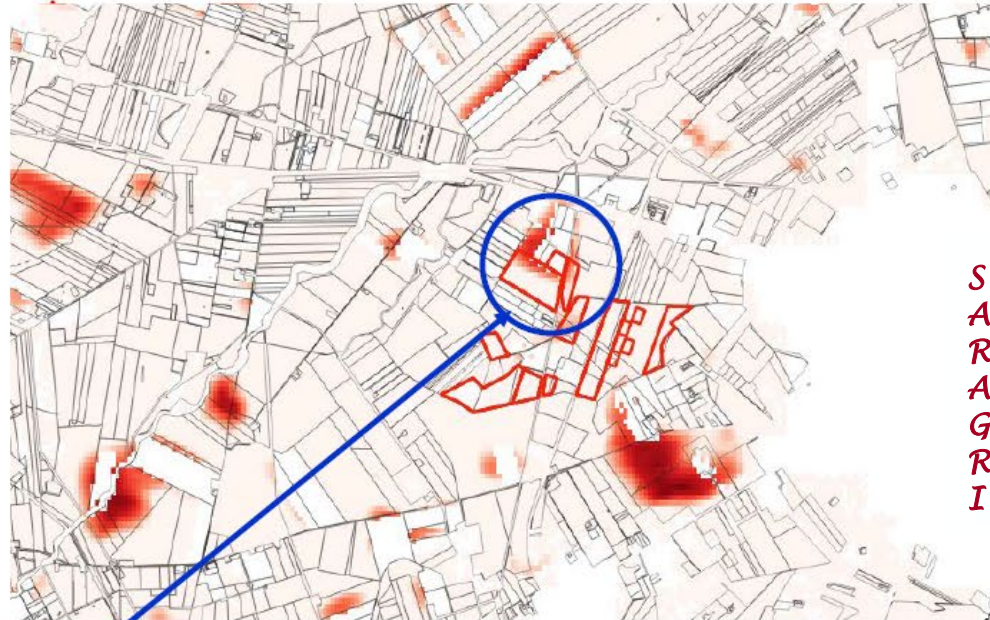
image courtesy: CNR-IREA, SARAGRI project

SARAGRI: Integrating incoherent & coherent change detection

image courtesy: CNR-IREA, SARAGRI project

COSMO Coherence @1 day
 CSG 14/09/2021
 CSK 15/09/2021
 DSC, 16:57 UTC

Sentinel-1 Coherence @6 days
 S-1 14/09/2021
 S-1 20/09/2021
 A146, 16:48 UTC



Tillage Disk harrowing (2): CREA_16, 15-Sept-21 / 16-Sept-21

Similar patterns of surface changes appear in both maps
 There are also differences (likely due to different time interval & sensitivity)

SARAGRI: tillage practices products

Apulian Tavoliere site (southern Italy)

Potential use: early estimation of the cultivated area of the winter or summer crops

S1- based seasonal cumulative map of agricultural practices 01/09 – 30/11/2021

S2 NDVI area estimated on 12/04/2022

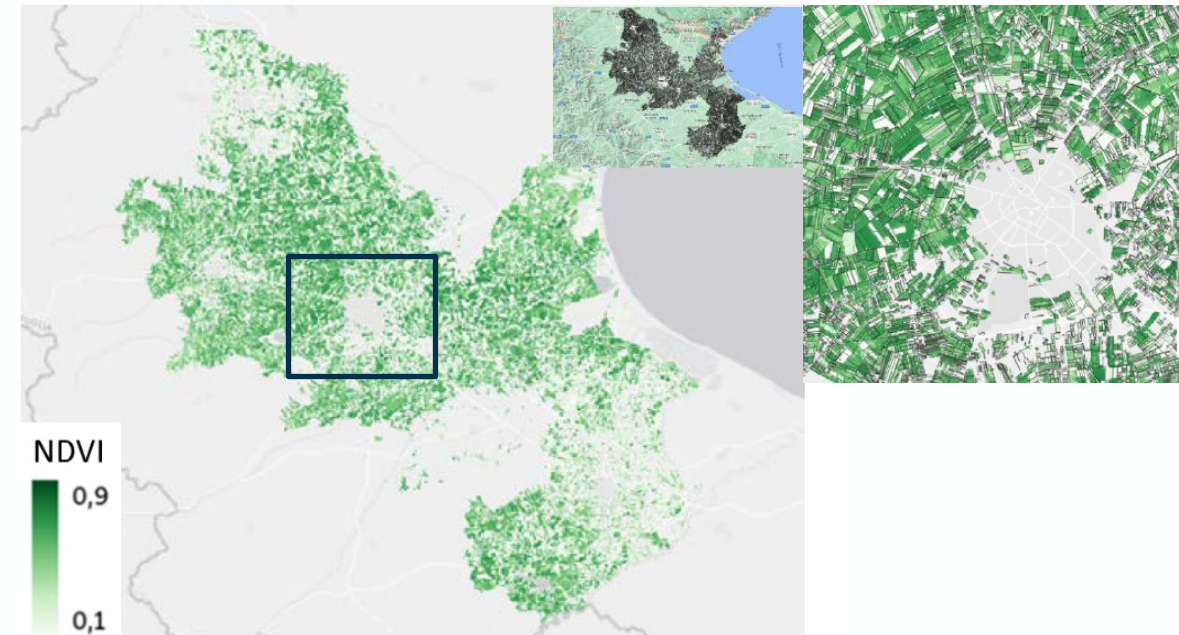
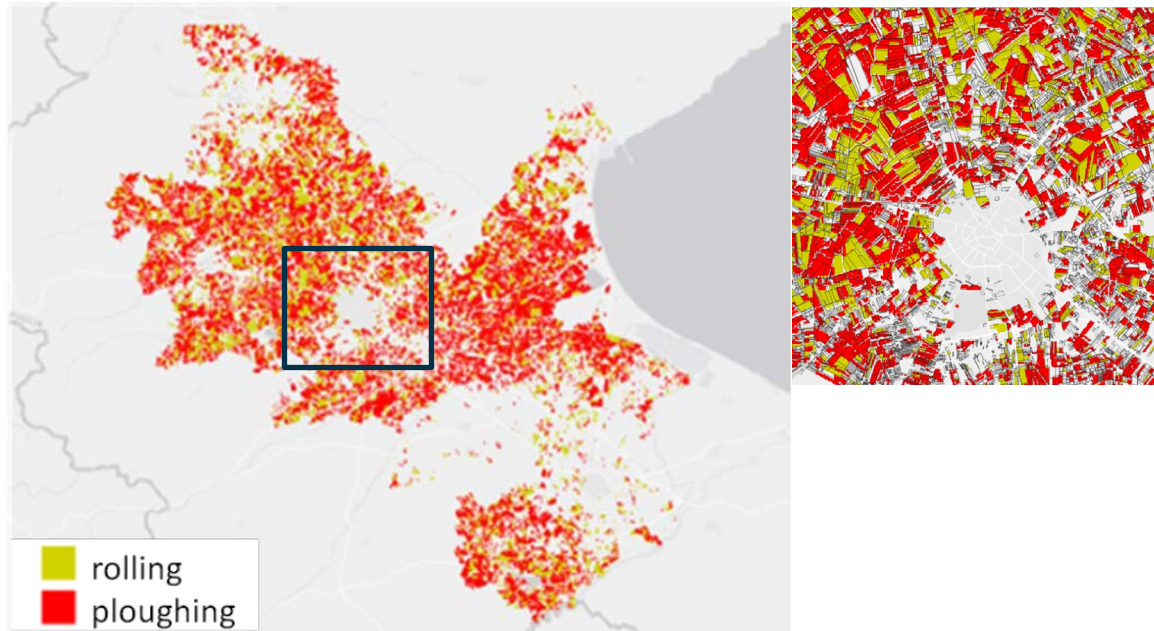
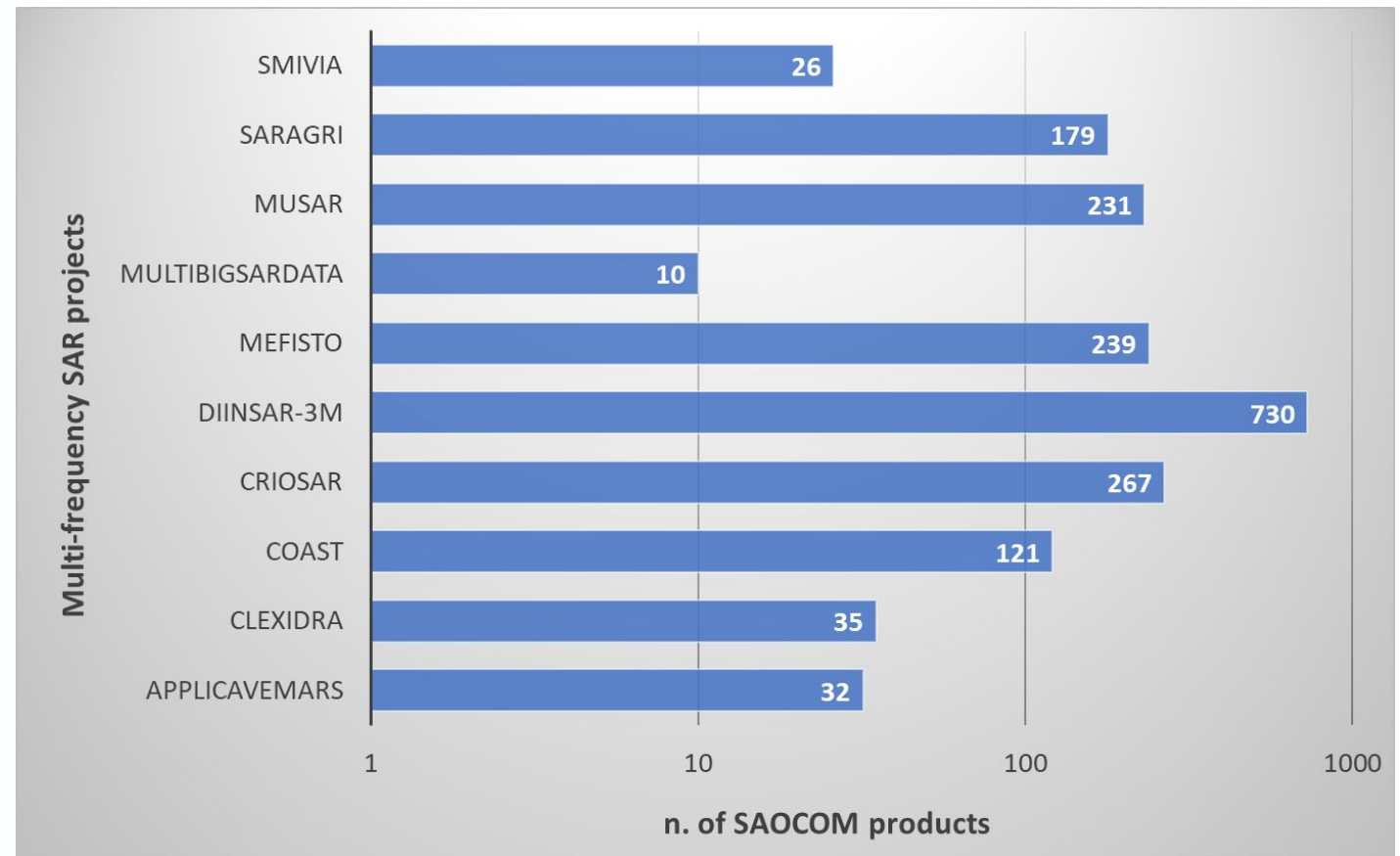


image courtesy: CNR-IREA, SARAGRI project

Achievements in SAOCOM data exploitation

- SAR MMF program was an opportunity for ASI to boost the exploitation phase of SAOCOM L-band data within the ZoE
- Total amount of products provided as of May 2023: [1870](#)
- After more than 1 year of implementation, at least 20 SAOCOM images per single geometry each AOI
- Best revisit times = 8 days in each geometry (i.e. SAOCOM-1A and 1B)
- Ad hoc acquisitions of quad-pol StripMap images. Benefits e.g. for model inversion and improvement of soil moisture retrieval (CLEXIDRA)



SARAGRI: Combining S1 & SAOCOM for SSM retrieval

- Interoperability of Sentinel-1 & SAOCOM platforms for SSM retrieval, to improve temporal resolution
- Dense time series of SAR data → incoherent short term change detection (5 and 3 days on average for Apulian Tavoliere and Jolanbda di Savoia, resp.)

Scatterplot of S-1 (orange squares) and SAOSOM (blue points) SSM vs. SSM observed over the Apulian Tavoliere and Jolanda di Savoia sites. Two outliers (3 sigma) are in black triangles. Line 1:1 in black

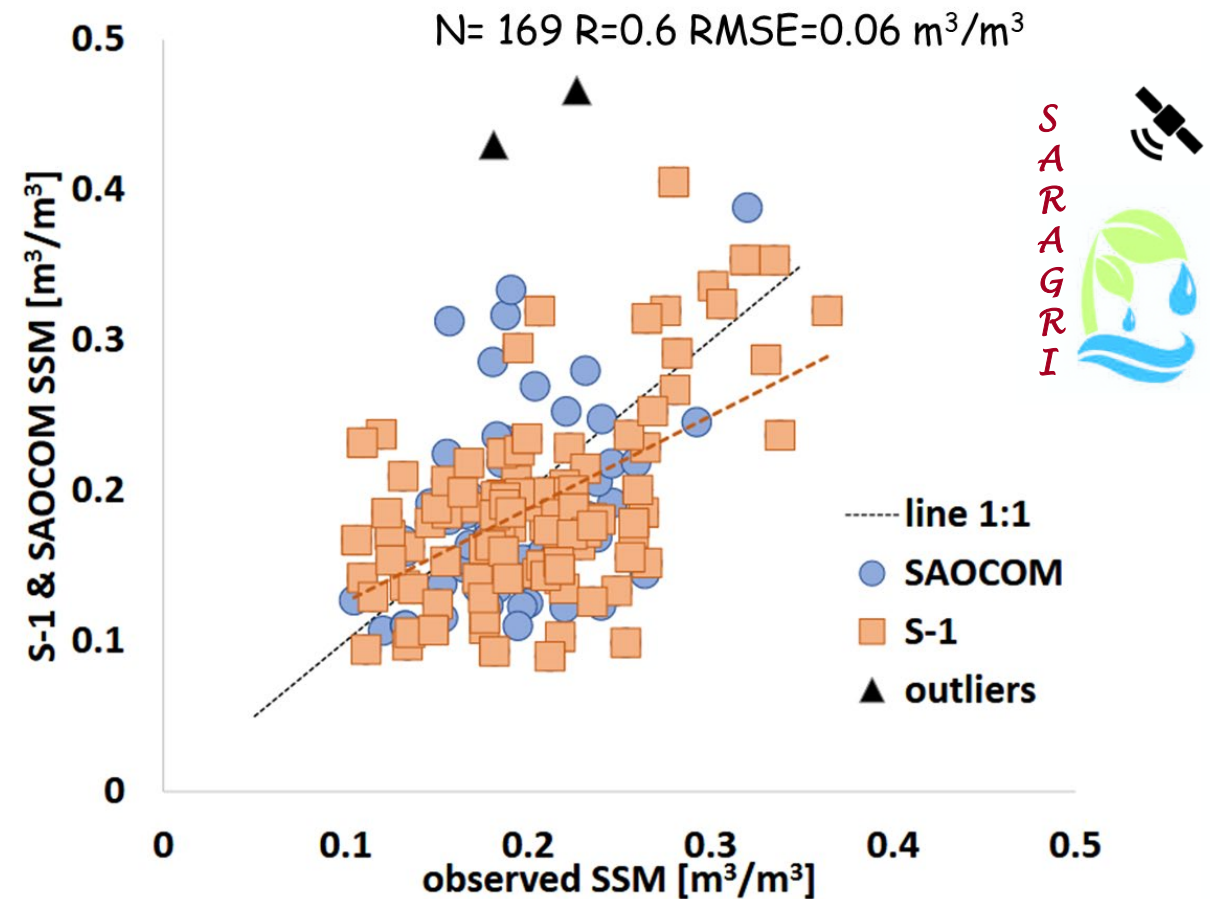
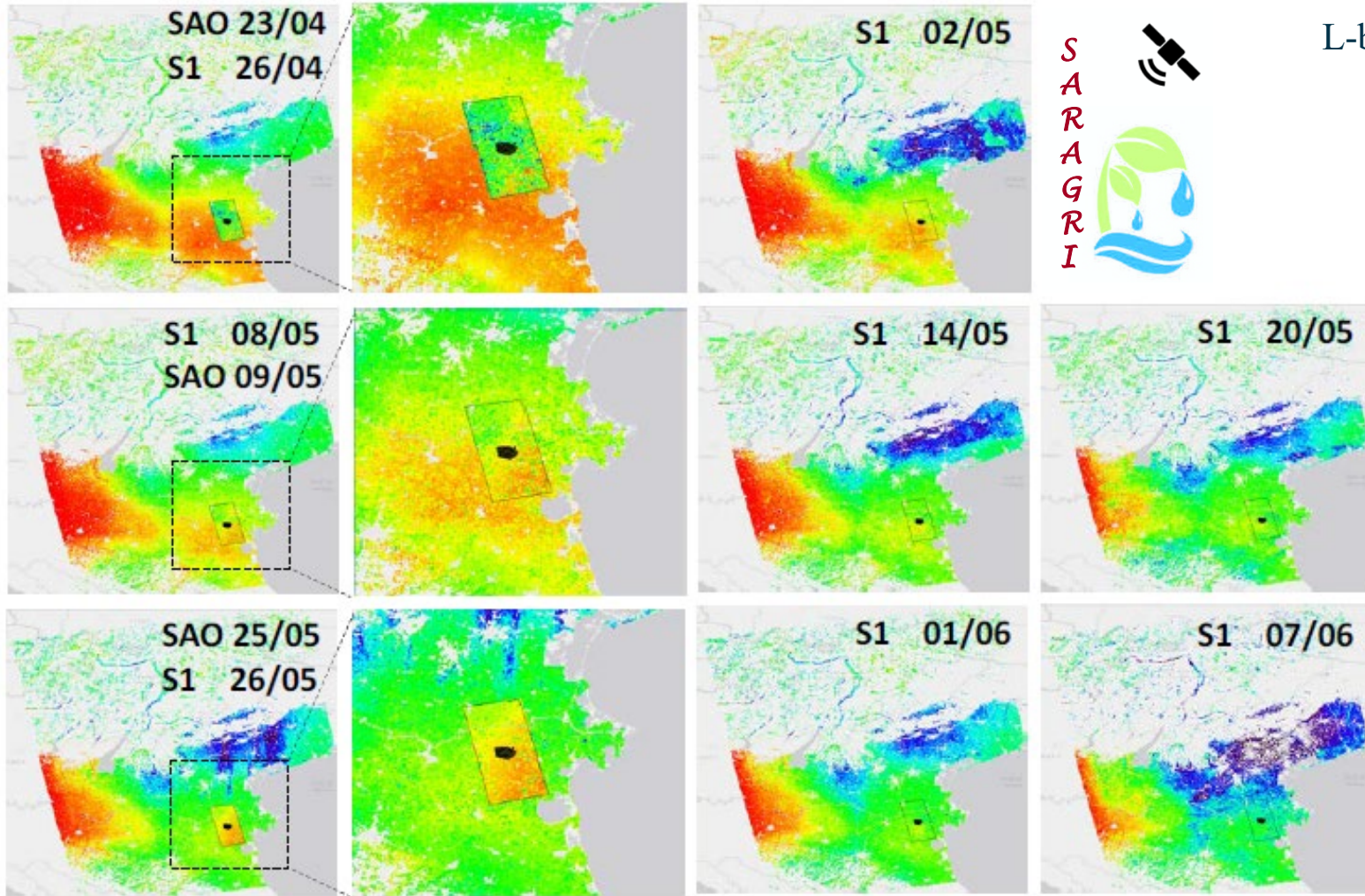


image courtesy: CNR-IREA, SARAGRI project

SARAGRI: Combining S1 & SAOCOM for SSM retrieval



L-band SAOCOM compared with C-band Sentinel-1

Time series of multi-frequency SSM maps derived from Sentinel-1 and A-SAOCOM between April and June 2020 over Jolanda di Savoia, Italy.

The SAOCOM SSM maps are superimposed over the closest Sentinel-1 SSM maps.

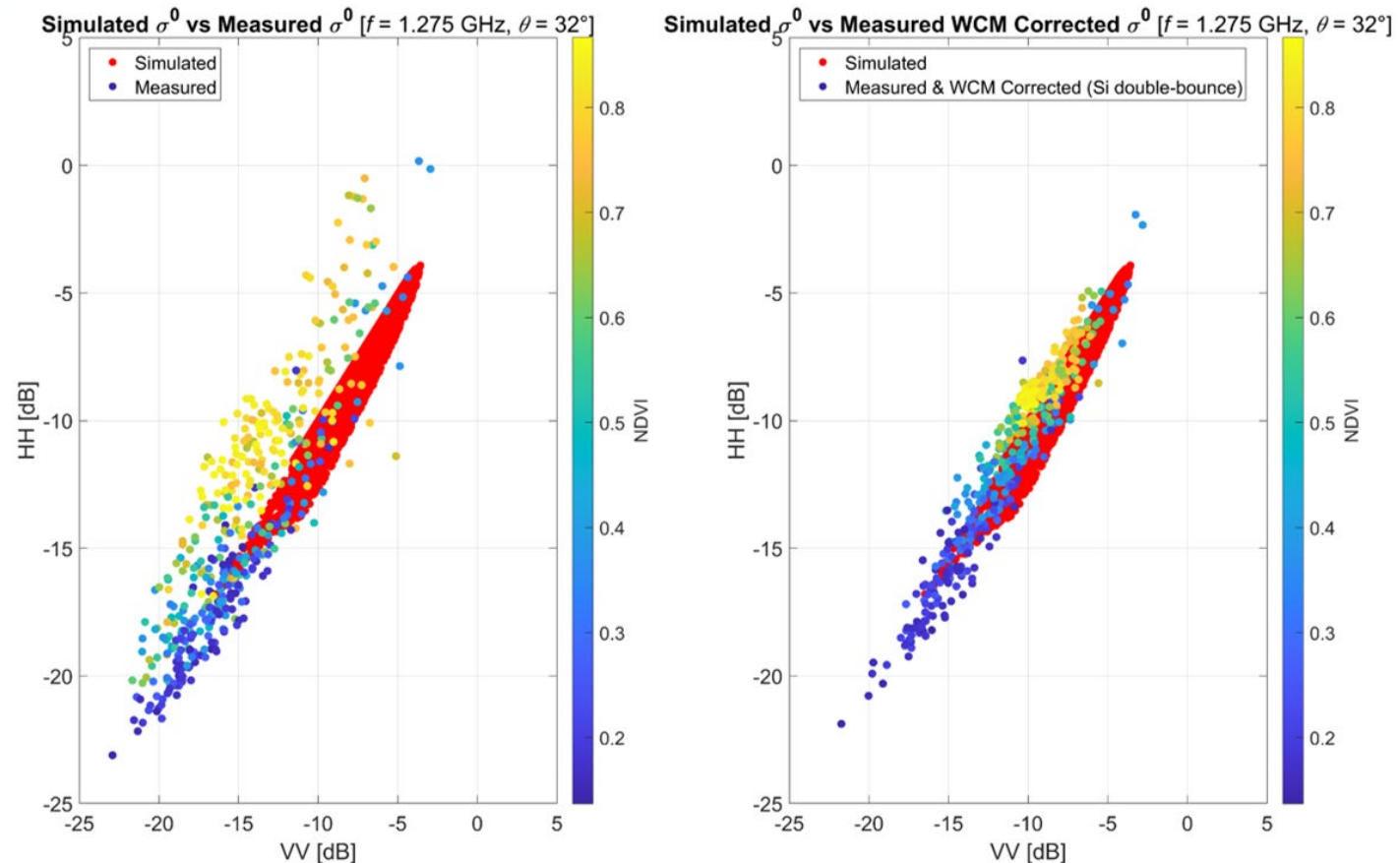
The black rectangle corresponds to the SAOCOM footprint

CLEXIDRA: SAOCOM SM retrieval vs. models

Objectives: Develop an automatic SM retrieval algorithm by means of bare and vegetated soil scattering models inversion, Bayesian minimization and machine learning techniques

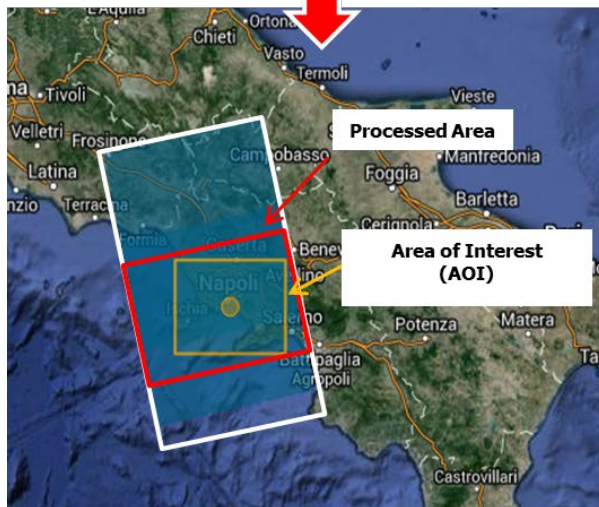
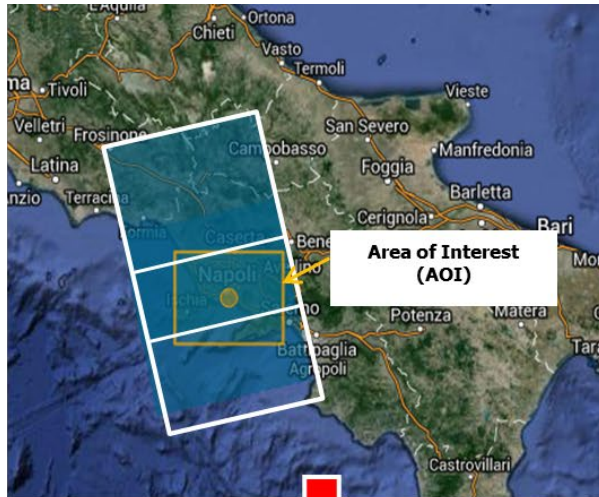
(left) for low NDVI values the data are in line with the model; however, both HH and VV co-polarized SAR backscattering coefficients are overestimated. For high NDVI values a deviation from the model is noted.

(right) the points characterized by high NDVI values tend to approach the values simulated by the model after the calibration of the Water Cloud Model (WCM) and after applying it to the SAR data in order to correct the effects of vegetation.



Comparison of soil scattering between data simulated by the Semi Empirical Model (SEM - red dots) and **SAOCOM dataset** acquired over the Monte Buey site (Argentina), corrected or not for vegetation effects with the Water Cloud Model (colored dots) (image courtesy: CLEXIDRA project).

DInSAR-3M: SAOCOM full processing InSAR chain



Block diagram of the implemented procedure related to the ingestion, merging and cut of the **SAOCOM L1A SAR data**.

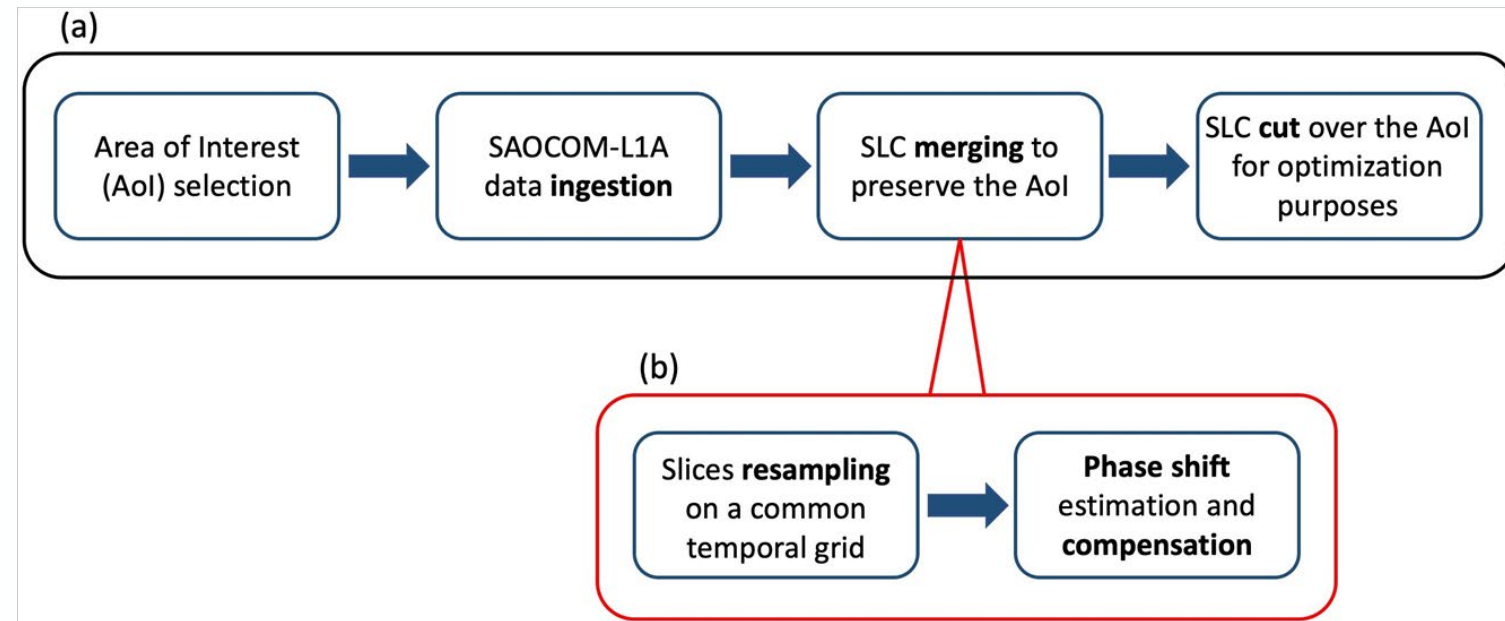


image courtesy: CNR-IREA, DInSAR-3M project

DInSAR-3M: SAOCOM full processing InSAR chain

Multiple-slice phase shift estimation and compensation

Acquisition dates: 01102021 & 17102021

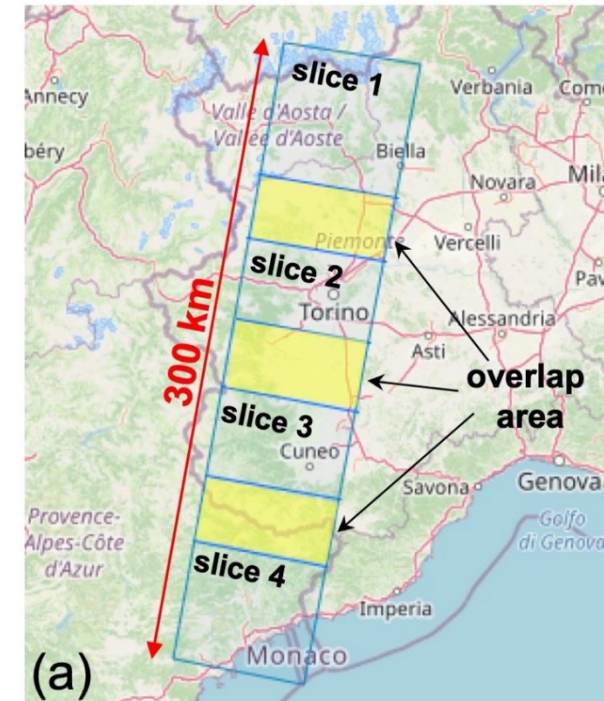
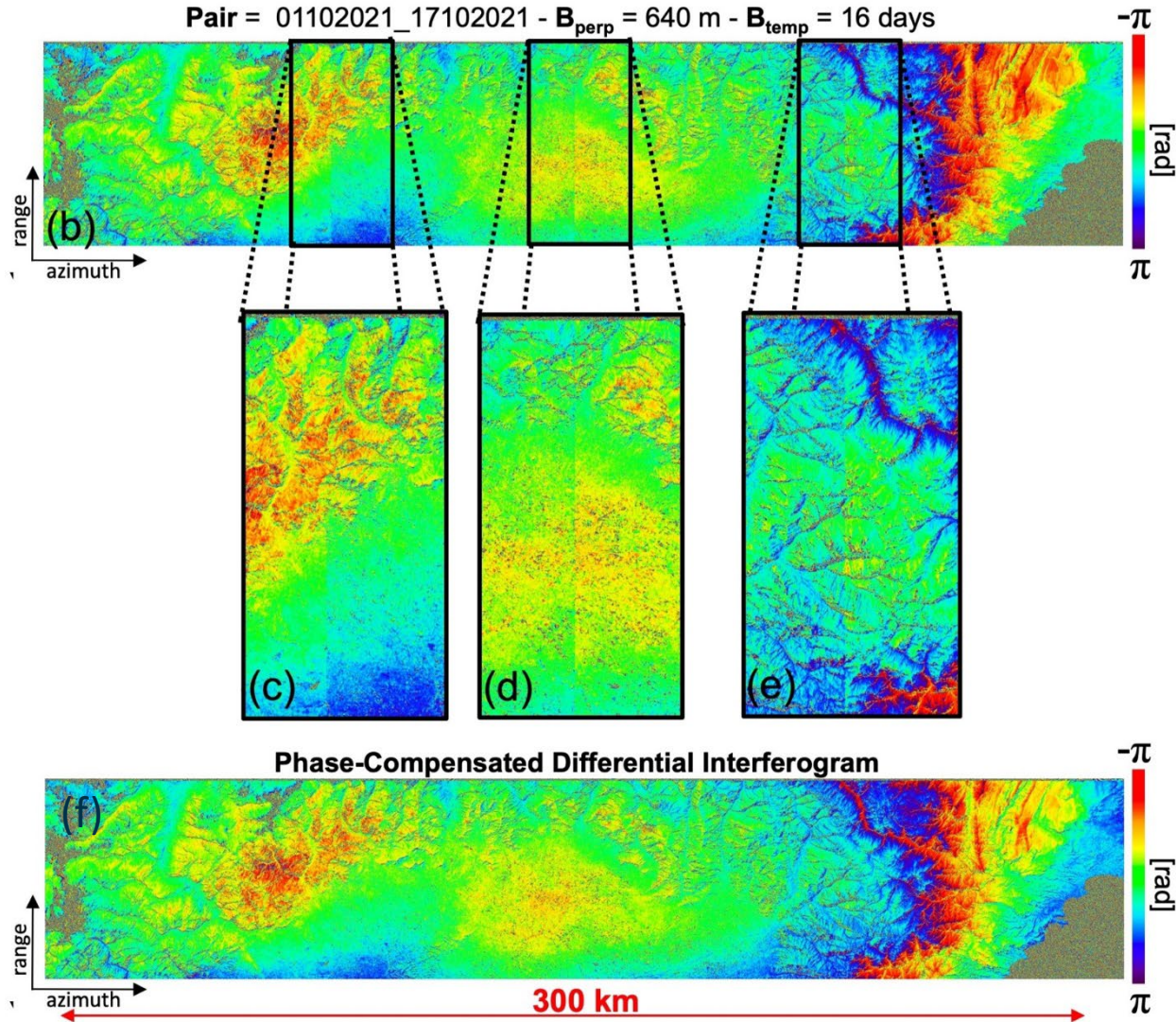
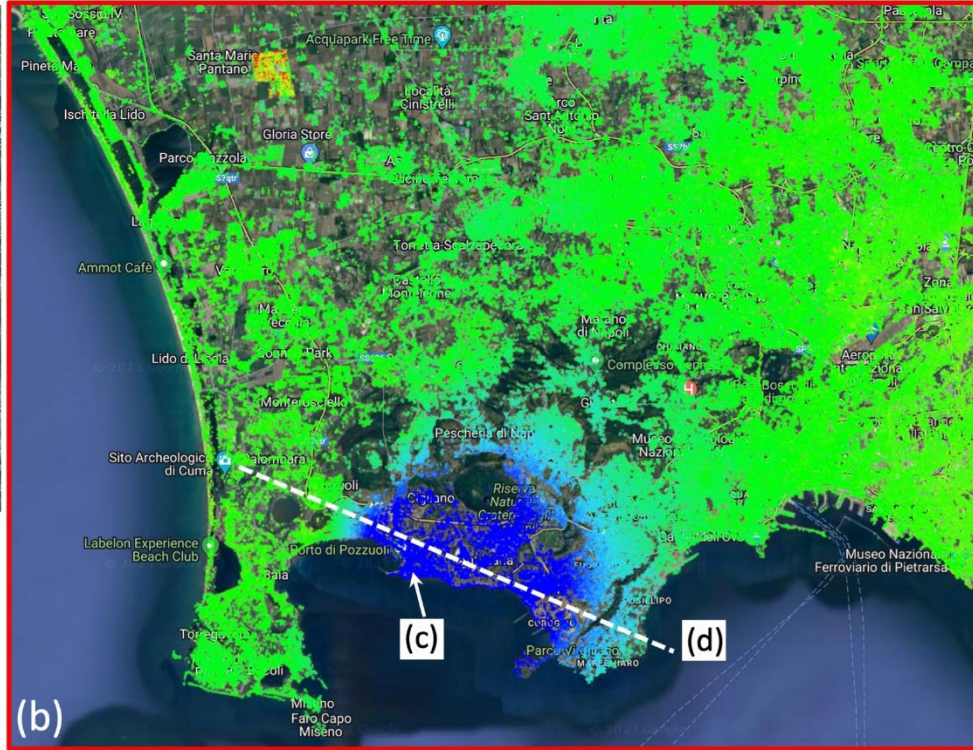
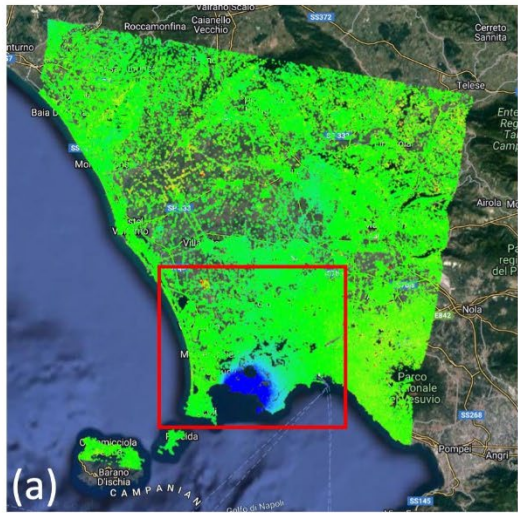


image courtesy: CNR-IREA, DInSAR-3M project

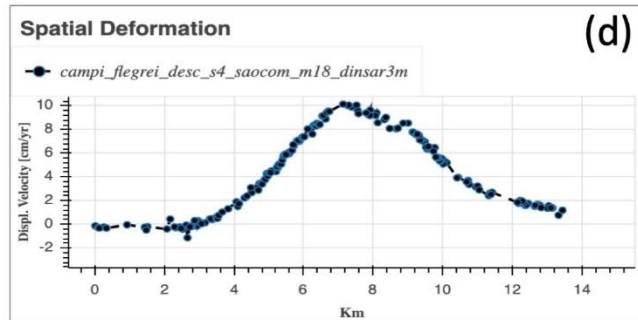
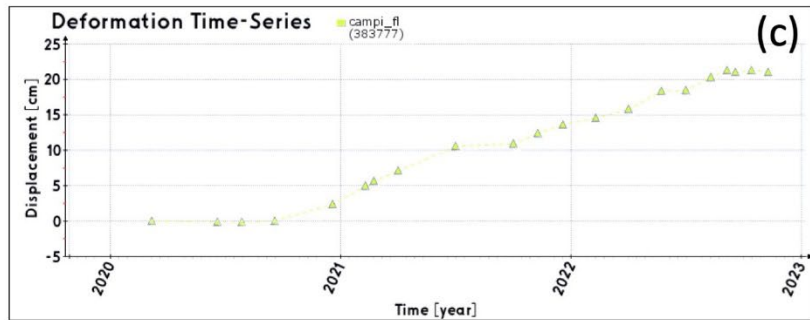
Pair = 01102021_17102021 - $B_{\text{perp}} = 640 \text{ m}$ - $B_{\text{temp}} = 16 \text{ days}$



DInSAR-3M: SAOCOM full processing InSAR chain



Descending (swath: S4, path: 108) SAOCOM-1 dataset (21 images) relevant to the Campi Flegrei caldera Aol: (a-b) overall mean deformation velocity map; (c) plot of the displacement time-series in a pixel located within the Pozzuoli harbour, which represents the area affected by the maximum of the displacement; (d) profile of the mean deformation velocity values along a section (white line).



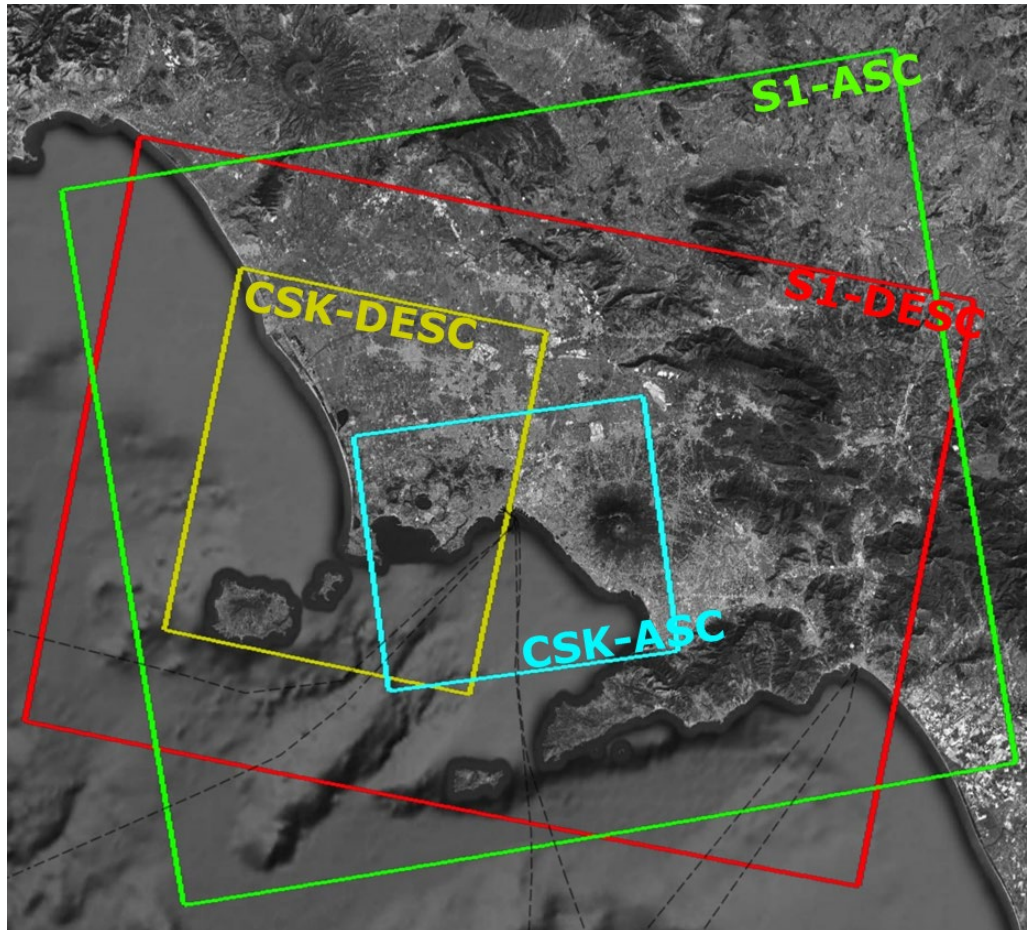
More details in the oral presentation by De Luca et al. @ FRINGE 2023

Tomorrow morning, Session 5.01.a: C-and L-band synergies: ESA-JAXA cooperation and beyond Time Location: Auditorium I

image courtesy: CNR-IREA, DInSAR-3M project



DInSAR-3M: Multi-frequency and multi-platform data integration



General expression

$$\begin{cases} v_{losA_1} = v_U \cos \vartheta_{A_1} - v_E \sin \vartheta_{A_1} \cos \alpha_{A_1} - v_N \sin \vartheta_{A_1} \sin \alpha_{A_1} \\ v_{losD_1} = v_U \cos \vartheta_{D_1} + v_E \sin \vartheta_{D_1} \cos \alpha_{D_1} - v_N \sin \vartheta_{D_1} \sin \alpha_{D_1} \\ \vdots \\ v_{losA_j} = v_U \cos \vartheta_{A_j} - v_E \sin \vartheta_{A_j} \cos \alpha_{A_j} - v_N \sin \vartheta_{A_j} \sin \alpha_{A_j} \\ v_{losD_j} = v_U \cos \vartheta_{D_j} + v_E \sin \vartheta_{D_j} \cos \alpha_{D_j} - v_N \sin \vartheta_{D_j} \sin \alpha_{D_j} \end{cases} \quad \text{with } 1 \leq j \leq M, j \in \mathbb{N}$$

Expression for SSO satellite platforms

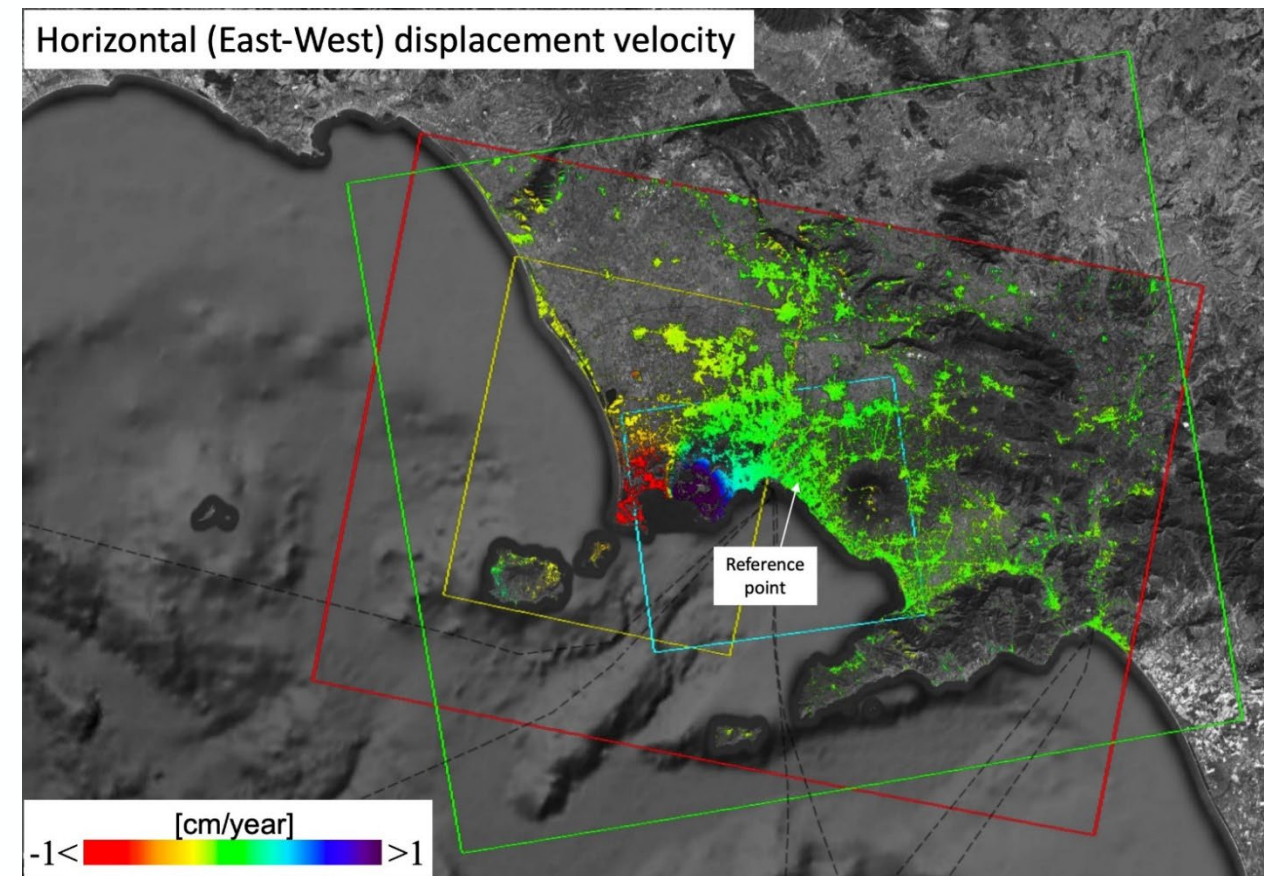
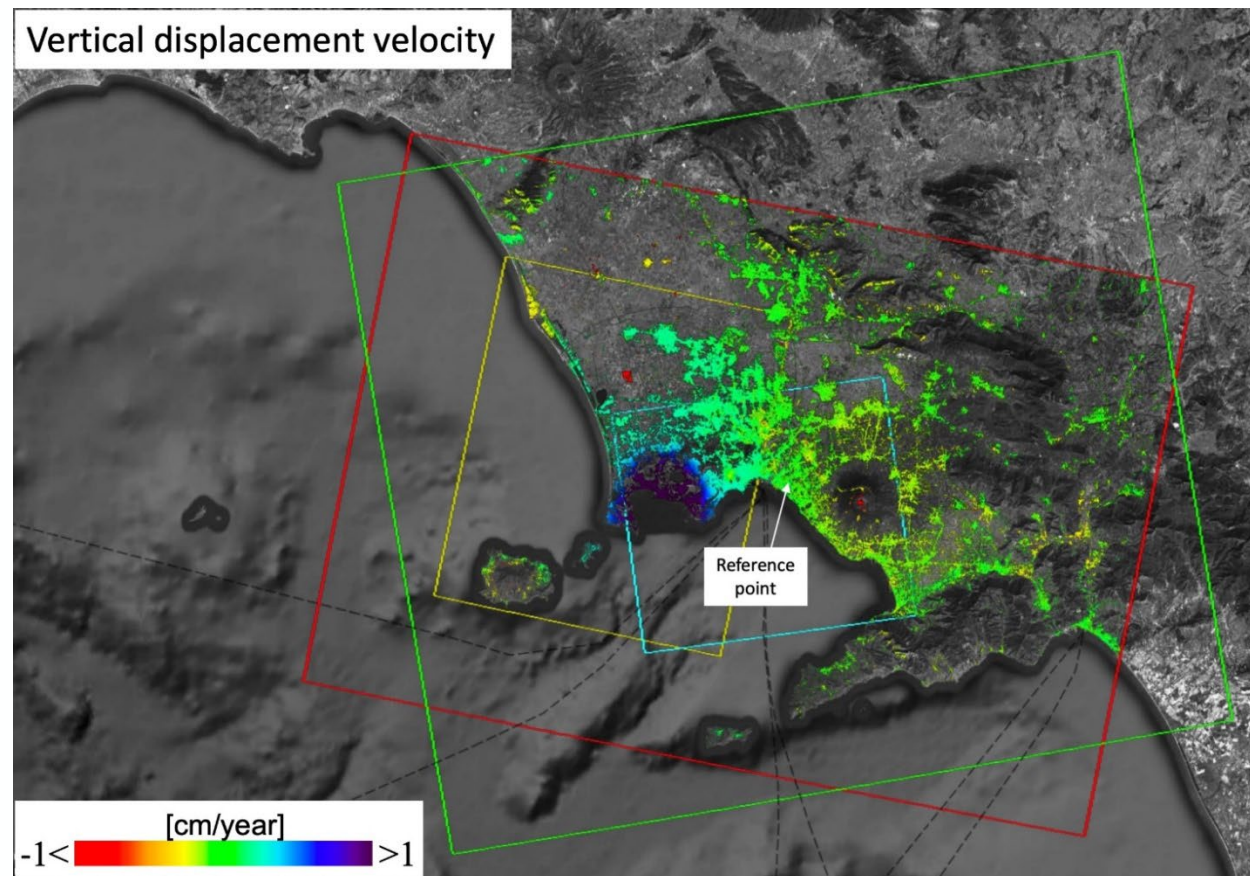
$$\begin{cases} v_{losA_1} = v_U \cos \vartheta_{A_1} - v_E \sin \vartheta_{A_1} \\ v_{losD_1} = v_U \cos \vartheta_{D_1} + v_E \sin \vartheta_{D_1} \\ \vdots \\ v_{losA_j} = v_U \cos \vartheta_{A_j} - v_E \sin \vartheta_{A_j} \\ v_{losD_j} = v_U \cos \vartheta_{D_j} + v_E \sin \vartheta_{D_j} \end{cases} \quad \text{with } 1 \leq j \leq M, j \in \mathbb{N}$$

image courtesy: CNR-IREA, DInSAR-3M project

DInSAR-3M: Multi-frequency and multi-platform data integration

(left) map of the retrieved vertical displacement component; (right) the corresponding horizontal one, which are single-point referenced.

As evident by observing the displacement components, the algorithm retrieves the deformation not only over the common geometric area, but also over the other areas where coherent pixels for at least two independent acquisition geometries are available.



MUSAR: Multi-frequency and multi-platform data integration

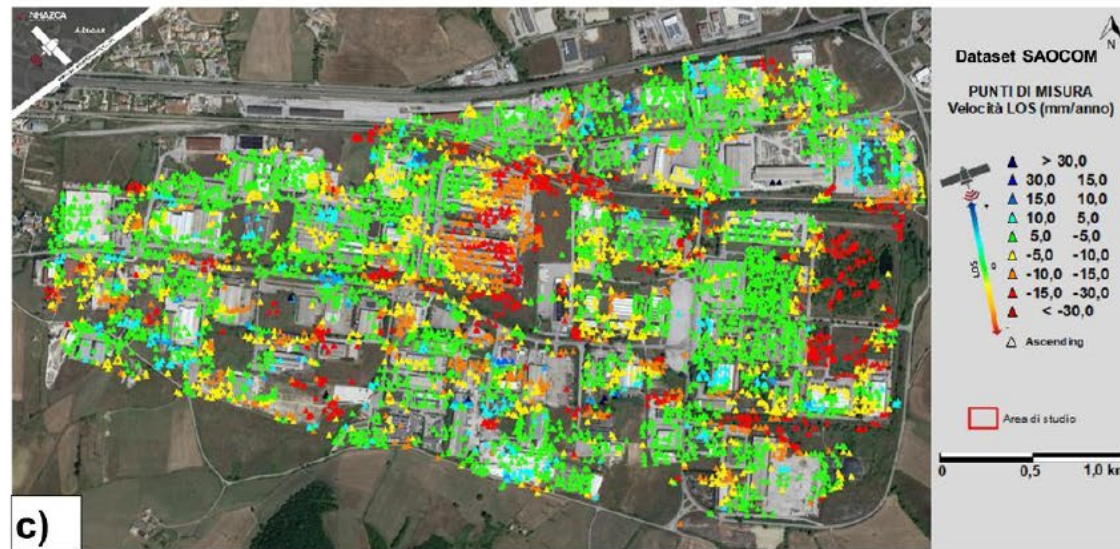


image courtesy NHAZCA S.r.l.,
MUSAR project

MUSAR: Multi-sensor InSAR data fusion

NHAZCA S.r.l. developed a mathematical model by which displacement components $f_i(X_p)$ ($i=1..3$) can be estimated in the generic point $X_p=(x_p,y_p,z_p)$ by integrating Photomonitoring measurements ($f_1(X_j), f_2(X_j)$) $j=1..M$ and the DLOS $_k(X)$ ($k=1..Q$) measurements, either DInSAR measurements or PS displacements, by using the linear equation system.

$$\begin{cases} f_i(X_p) + \nabla f_i(X_p)\Delta X = f_i(X_j), & i = 1..2, \quad j = 1..M \\ D_{LOS}^k(X_p) + \nabla D_{LOS}^k(X_p)\Delta X = D_{LOS}^k(X_{S_d}), & k = 1..Q, d = 1..D \end{cases}$$



$$Al = u$$

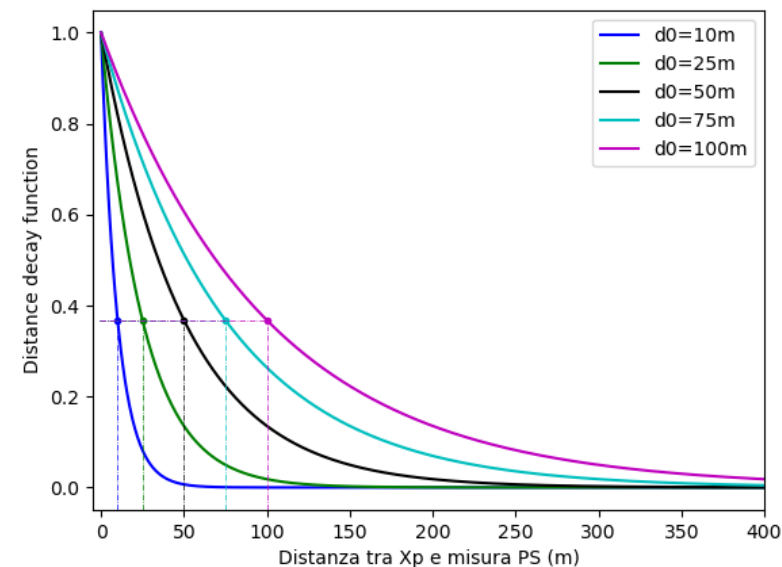


The solution is achieved by Weighted least squares (WLS) method $\hat{l} = (A^TWA)^{-1}A^TWu$

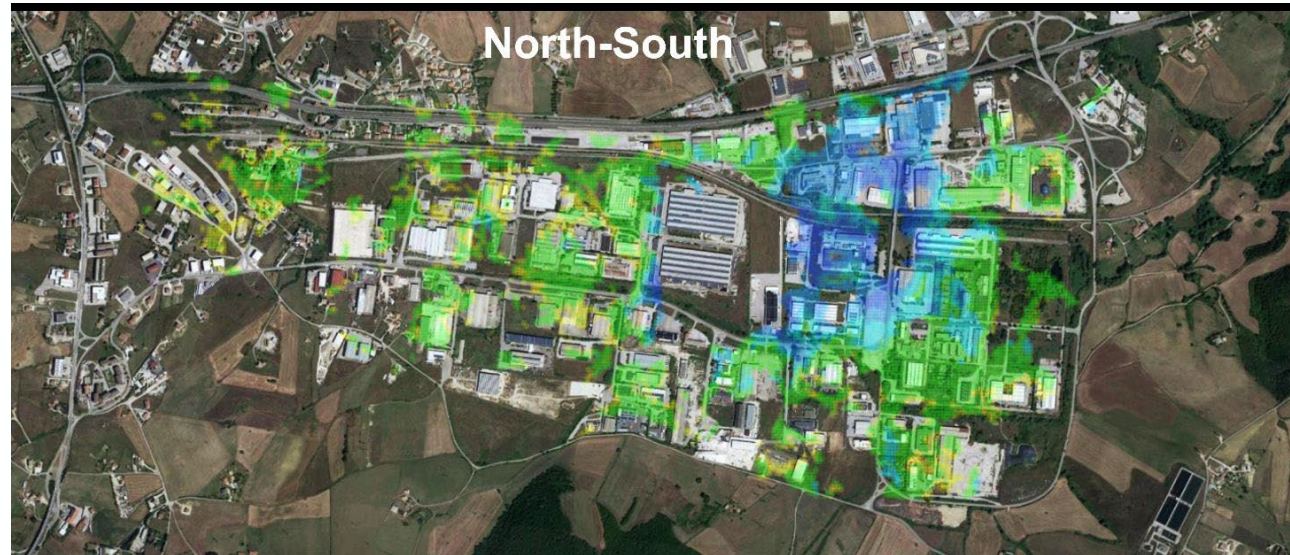
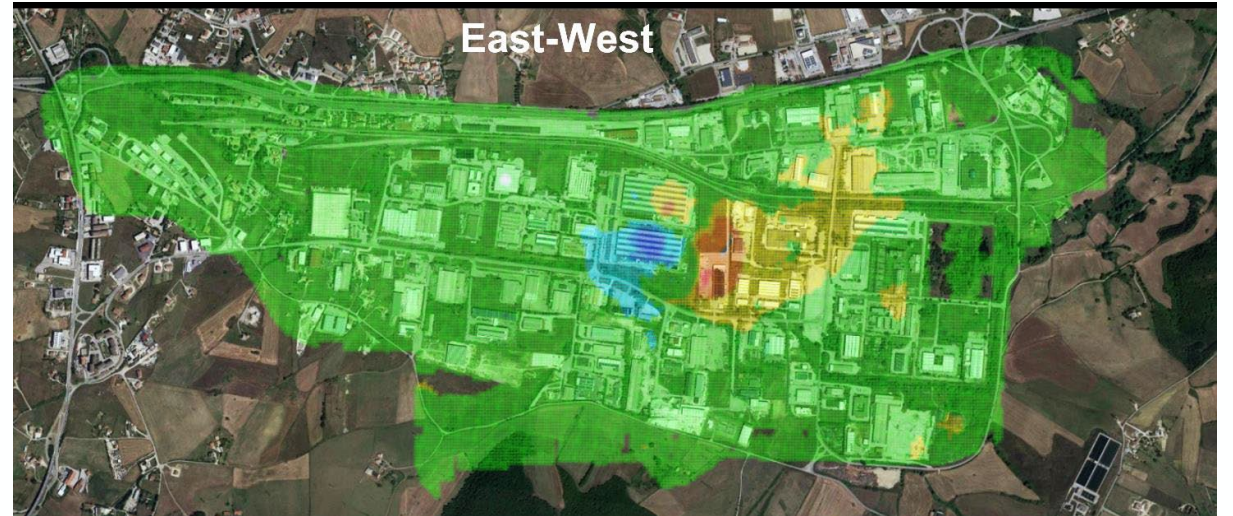
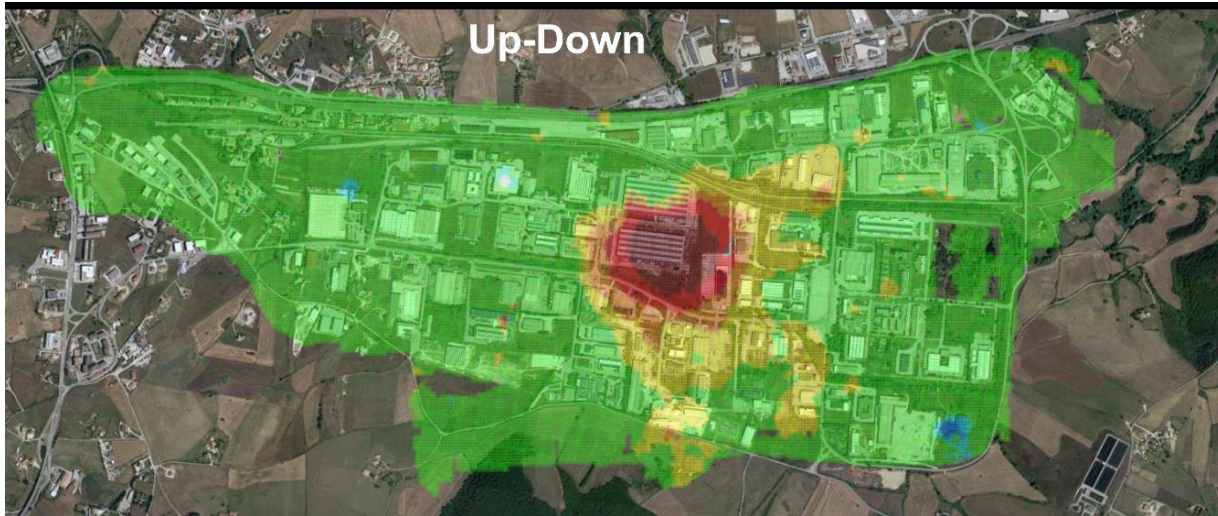
A decay constant of used distance is introduced to weigh the contribution that each PS measurement brings to the 3D components estimate according to the exponential formula

where $f(d_i) = e^{-\frac{d_i}{d_0}}$

- d_i is the distance between the PS measurement PS_i and X_p is the point where the estimate is determined
- d_0 is the location



MUSAR: Multi-sensor InSAR data fusion



Estimation of 3D displacement components achieved through data fusion of COSMO-SkyMed and Sentinel-1 Persistent Scatterers in a built-up area in Tito Scalco, Potenza (Italy) affected by subsidence. (image courtesy NHAZCA S.r.l., MUSAR project).

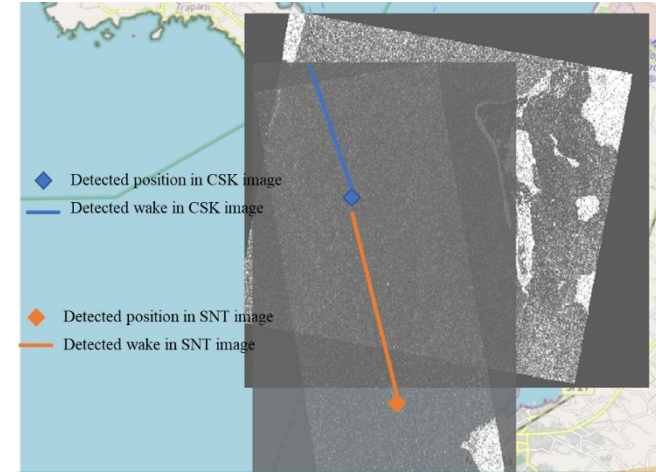
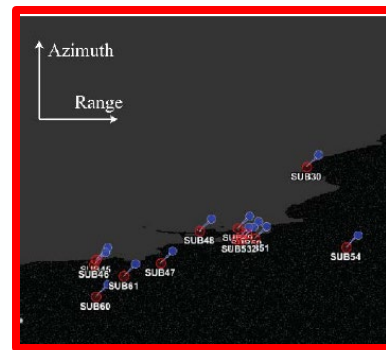
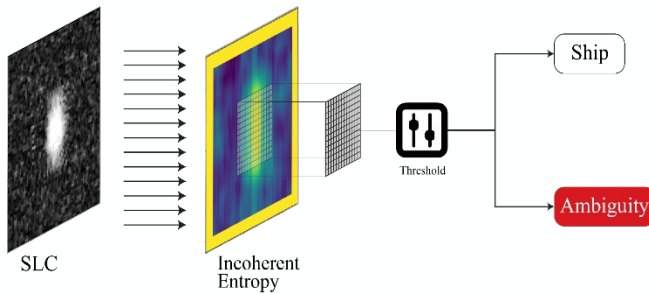


More details in the poster by Belcecchi et al. @ FRINGE 2023

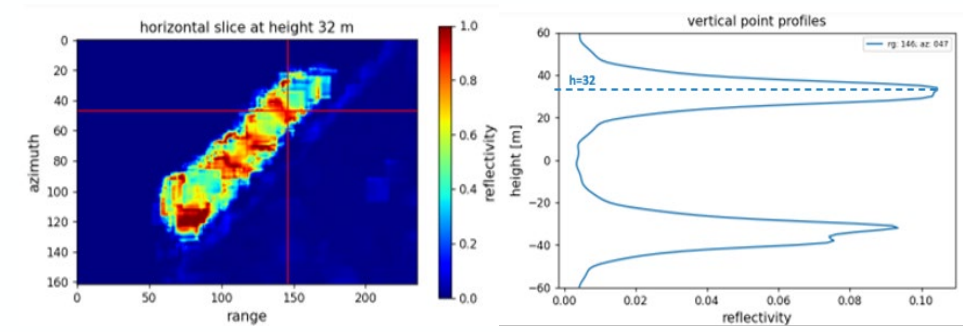


COAST: SAR-based ship detection

- **Partners:** Federico II" Napoli Univ. (UNINA), Euro.Soft srl
- **Objectives:** Improve multi-frequency and multi-polarimetric ship detection algorithms based on target related properties.



Results of ship-wake detection algorithm based on Radon Transform, applied to multi-temporal CSK and Sentinel-1 SAR images.



Tomographic profile of Diamond Princess ship, gathered with TomoSAR processing of CSK dataset.

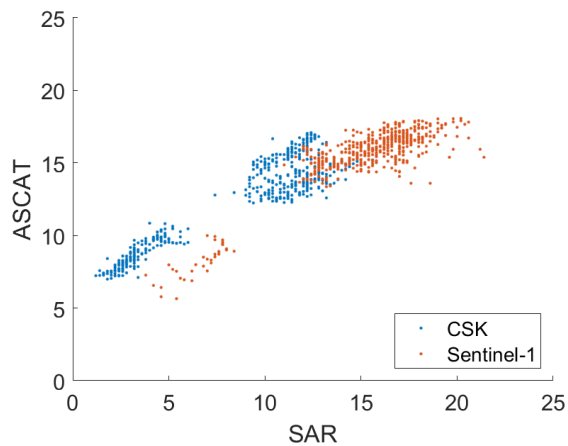
Results on the ship detection pipeline (CFAR approach, Sub-Look Analysis and Incoherent Entropy) applied to CSK (BLUE), SAOCOM (GREEN) and Sentinel-1 (RED) data: red points correspond to identified targets. Product produced from Original SAOCOM Product - ©CONAE – COMISION NACIONAL DE ACTIVIDADES ESPACIALES (2020-2021)

Images courtesy DII-UNINA, COAST project

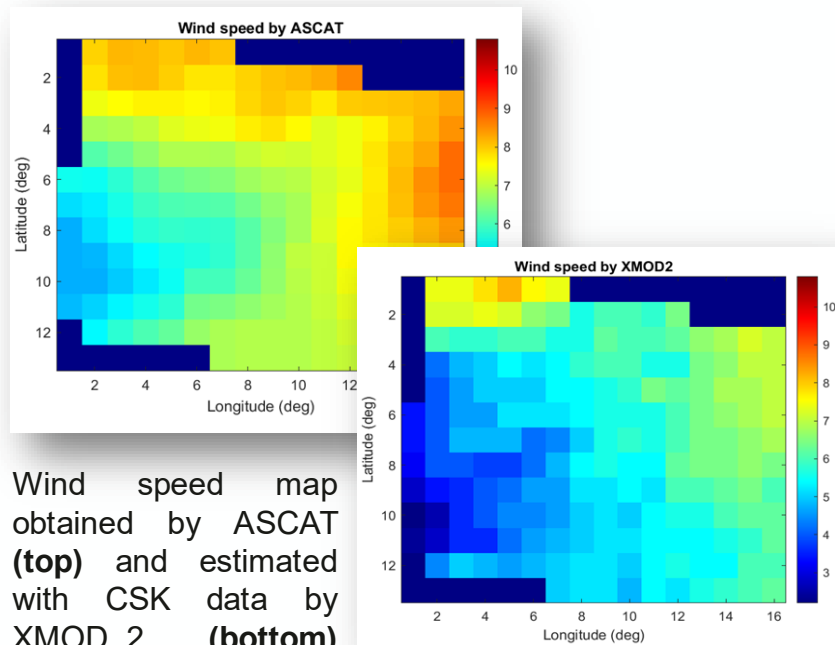
APPLICA VEMARS: SAR-based wind field estimation



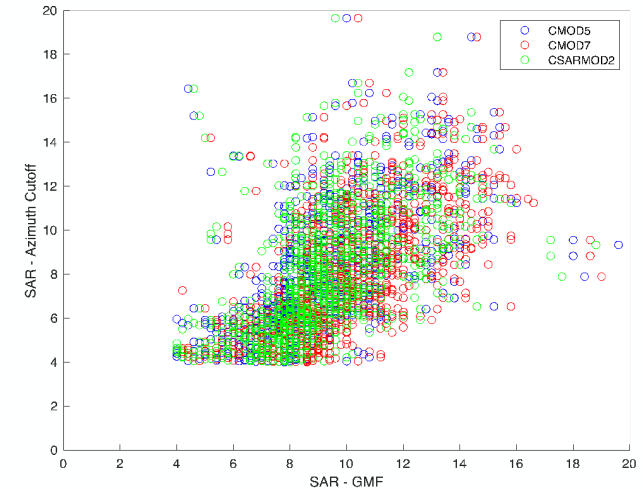
- **Partners:** Parthenope” Napoli Univ. (UNP), CNR-ISP, ICM-CSIC
- **Objectives:** develop, verify and ameliorate GMF algorithms to estimate wind field from SAR imagery at different spectral bands, also improving product validation and cross-comparison phases.



Scatterplot to contrast SAR retrievals (blue and red spots stand for CSK and S1, respectively) with ASCAT reference wind, for dataset collected in North Sea



Wind speed map obtained by ASCAT (**top**) and estimated with CSK data by XMOD_2 (**bottom**) using the ASCAT wind direction



GMF	Azimut Cut-Off		
	CRMSD	BIAS	CORR
CMOD5	1.7799	1.1378	0.5840
CMOD7	1.8073	1.8172	0.5783
CSARMOD2	1.7894	1.1501	0.5691

Scatterplot to contrast S1 winds retrieved using azimuth cut-off with the GMF ones.

Images courtesy Parthenope University, APPLICA VEMARS project



Highlights, conclusions & future perspectives

- The SAR MMF program allowed consortia to develop mature and validated chains for processing [SAOCOM data](#), paving the way [towards a more routine and systematic use of these L-band data](#), e.g. for civil protection and disaster risk management purposes;
- In the longer-term perspective, the national community will be best placed to exploit L-band SAR data from future satellite missions (e.g. ROSE-L and NISAR), taking benefits of test-bed and expertise gained within ASI's SAR MMF program;
- In [agricultural](#) applications, [ground motion](#) assessment and [cryosphere](#), L-band SAR data proved crucial to retrieve crop/vegetation properties, identify deformation patterns caused and retrieve snow properties;
- Concerning [maritime](#) applications, ship detection pipelines were successfully assessed in case of visible and non-visible ships, taking benefits of multi-frequency SAR products provided as single and joint acquisitions;
- Concerning [marine](#) applications, L-, C- and X-band Geophysical Model Functions (GMFs) were properly tested over Sentinel-1, CSK/CSG and SAOCOM data, with improvements obtained at C- and X-band by exploiting wind direction directly from the SAR scene;

Highlights, conclusions & future perspectives

- For purposes of SAR data integration and urban changes analyses, all the above described applications demonstrated that acquisitions collected at different wavelengths with short temporal time span, if not even co-located, are very advantageous.
- These types of SAR datasets, however, can be achieved through a coordinated satellite tasking that can be addressed at the space agency's level only, and making the best out of bilateral cooperation and virtual constellation approaches.
- According to the ASI's roadmap for scientific downstream applications, the outputs of the SAR MMF program will form the basis/input for proper demonstrators wherein they can be exploited operationally, to address specific needs expressed by the user community and/or institutional stakeholders
- The SAR MMF acts as a foundational step of the ASI's "Innovation for Downstream Preparation" (**I4DP**)

Thank you for your attention!

Bradford

Leeds

For further information:

Deodato Tapete (deodato.tapete@asi.it)

Antonio Montuori (antonio.montuori@asi.it)

FRINGE 2023

University of Leeds, UK | 11 - 15 September 2023



Agenzia Spaziale Italiana